Progress In Electromagnetics Research, Vol. 164, 17–25, 2019

Design and Experimental Validation of Multifunction Antenna with Direct Modulation for Radar and Communication

Samir Ouedraogo[1], Israel D. Hinostroza Sáenz[1, *], Régis Guinvarc'h[1], and Raphaël Gillard[2]

Abstract—A multifunction antenna system providing a radar function and a communication function simultaneously is proposed. The system is composed of a horn antenna whose feeding waveguide is loaded with slots. The horn radiation is used for the main radar function. The slotted waveguide radiation is controlled independently from the horn radiation to perform a direct binary phase shift keying (BPSK) communication provided that each radiating slot is equipped with a simple switching mechanism. Then, the antenna system provides two different functions using orthogonal polarizations and directions. Measured results show 9.1 dB and 32 dB isolation between the two functions at the working frequency. In addition, the proposed system can be integrated with the existing radars which use horns by replacing only the feeding waveguide.

1. INTRODUCTION

In airborne platform, various radio systems such as communication, navigation or radar have to coexist with severe space constraints [1, 2]. Furthermore, each of them may require several radiating elements. This leads to the need for multifunction antenna systems sharing the same radiating aperture in order to achieve multiple applications [3, 4].

In [5, 6], system approaches are proposed that enable integrating radar and communication together, whereas solutions in [7–9] are focused on the antenna architecture itself. In [7], polarization diversity is used to achieve 45 dB isolation over a 20% band for a linear frequency modulation radar with communication capabilities (S-band). In [8], a slotted waveguide with slots milled into opposite walls is demonstrated to provide a high-gain solution for two signals with orthogonal polarizations at two different frequencies (S-band for radar and C-band for communication). However, all these solutions usually require two different feeding networks to route the communication and radar signals to the radiating structure, which may be seen as a drawback regarding the overall compactness.

On the other hand, direct modulation at the antenna level [10, 11] is an attractive solution to generate a communication signal from a transmitting antenna driven by a single unmodulated carrier. Furthermore, as the phase and magnitude of the modulated fields are radiated coherently in desired directions only, this can provide a very discrete communication link, which is highly relevant when combined with a radar application. In [9], benefit was taken of the Time Modulated Array (TMA) technique [12] to generate a modulated communication signal from a 16-monopole array primarily dedicated to radar operation. By conveniently switching the active dipoles, the main lobe was kept unchanged (preserving the radar function) while a low data-rate communication could be established in desired directions. However, a switching mechanism is needed for all elements in the array.

In [13], we proposed a new antenna system, which is a more compact solution than [9], by using a single radiating horn (commonly used in radar [14, 15]) instead of antenna array. Preliminary simulations

Received 18 June 2018, Accepted 3 October 2018, Scheduled 8 January 2019

* Corresponding author: Israel David Hinostroza Sáenz (israel.hinostroza@centralesupelec.fr).

[1] CentraleSupélec, SONDRA, Gif-sur-Yvette, France. [2] INSA-Rennes, Rennes, France.

have demonstrated its capability to achieve simultaneously radar and communication functions using a single input source. In this paper, a deeper insight in the design process is given, and a full characterization is provided, supported by experimental measurements.

The system is composed of a horn antenna fed through a single waveguide port, thus offering extreme simplicity and direct compatibility with many existing systems. The system is intended for transmission applications and the only RF input of the system is the radar signal at the level of the waveguide. The horn antenna is used for the radar function and it radiates a high-power directive beam in the x-direction. For the communication function, a couple of slots is milled in the top face of the waveguide. The communication signal is directly applied as the command to a switching mechanism to activate one of the slots at a given time in order to control the modulation (phase modulation in the present work) of the radiation at the level of the slot. A small fraction of the input power in the feeding waveguide is then radiated through the activated slot thus providing a communication link in the z-direction. As we will see later, BPSK direct modulation can be achieved thanks to this switching mechanism. This very simple antenna system provides 9.1 dB and 32 dB isolation between the two functions at the resonant frequency (5 GHz) in respectively communication and radar directions.

The paper is organized as follows: in Section 2, the antenna system design procedure is introduced explaining the working mechanism of the proposed solution. In Section 3, the performances of the antenna system obtained in simulation with FEKO [16] are analyzed. The proposed horn antenna is fabricated and the measured results are compared to those of simulations in Section 4. Note that the same principle could be used to achieve more advanced modulation schemes. For instance, QPSK may be achieved by using 4 switchable slots instead of 2.

2. MULTIFUNCTION ANTENNA DESIGN

The proposed multifunction antenna (Figs. 1 and 2) is made from a standard pyramidal horn antenna operating at 5 GHz. It produces a directive beam with linear z-polarization at ($\theta = 90°$; $\phi = 0°$), that is well-suited for a high-gain radar application.

Two identical slots ($L = 25.6$ mm and $l = 1.5$ mm) are milled in the upper wall of the feeding waveguide with the objective to radiate a fraction of the incident power in $\theta = 0°$ direction. This leakage mechanism aims at creating a communication link in addition to the main radar function. As the slots are longitudinal to the waveguide axis, the associated radiated field is y-polarized, which means

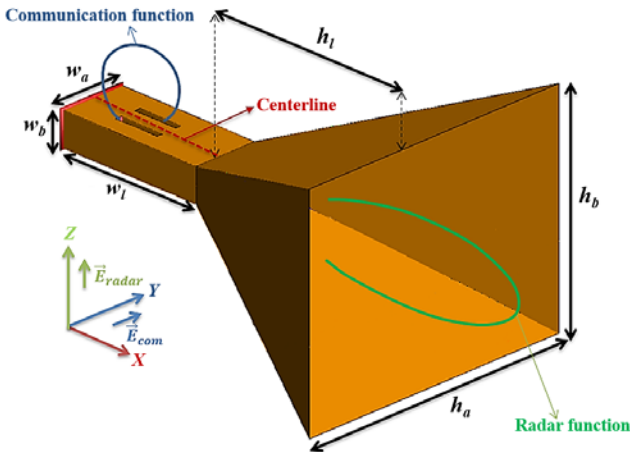

Figure 1. Antenna system at 5 GHz ($w_a = 47.55$ mm, $w_b = 22.15$ mm, $w_l = 135.2$ mm, $h_l = 151.34$ mm, $h_a = 180.95$ mm, $h_b = 125.81$ mm).

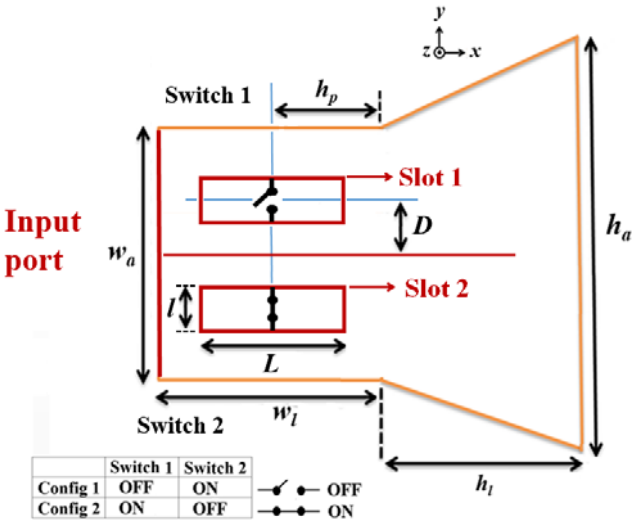

Figure 2. Configuration of slots (for antenna system of Fig. 1) for communication function ($L = 25.6$ mm, $l = 1.5$ mm, $D = 12.5$ mm, $h_p = 38.6$ mm).

radar and communication functions involve both orthogonal polarizations and directions for enhanced isolation.

The offset to the waveguide centerline, D, is used to control the leakage from the slot and thus the amount of incident power devoted to the communication function. Subsequently, it also defines the associated loss for the radar function. As an illustration, Fig. 3 depicts the decrease of the horn gain versus D. In practice, D has to be defined as a trade-off between radar loss and communication gain and thus depends on the target application. In the present design, D is arbitrarily set to 12.5 mm, which corresponds to a 1.3 dB gain drop for the horn antenna compared to the same structure without any slot.

In the present design, the communication function consists of a direct BPSK modulation of the y-polarized field in the xOz plane. It is obtained by activating only one of the two slots. Indeed, as these slots are placed symmetrically with regards to the waveguide centerline, a 180° phase jump in the radiated field is achieved each time the activated slot is changed [18]. This defines two complementary configurations (Fig. 2). In configuration 1, only slot 1 radiates while slot 2 is closed. Configuration 2 corresponds to the reverse situation. At this stage, we did not implement any actual switching mechanism but the one presented in [19] could be used quite straightforwardly for up to moderate power applications. For the sake of simplicity, only the activated slot is present in simulations (the other one being completely closed with PEC).

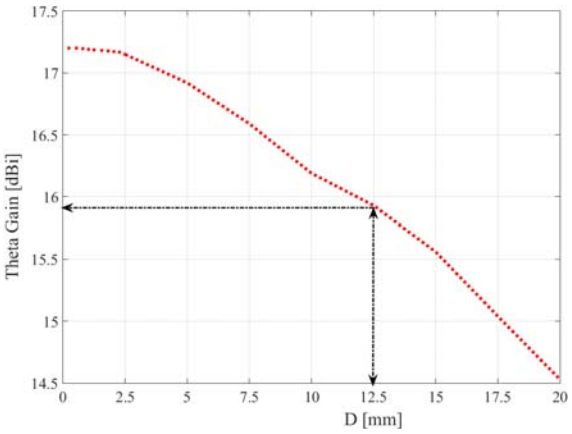

Figure 3. Simulated theta gain (radar function) versus offset D for one active slot ($\theta = 90°$, $\phi = 0°$, $f = 5$ GHz).

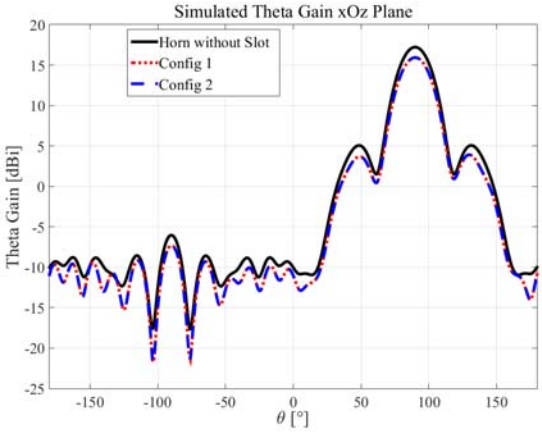

Figure 4. Comparison of simulated theta gains (radar function) in xOz plane at 5 GHz.

3. SIMULATED RESULTS

3.1. Radar Function

In this section, the simulated performance of the radar antenna is discussed. To speed up the simulations, in this section we consider zero thickness for the metallic walls. Fig. 4 presents theta gain in xOz plane for configurations 1 and 2. For comparison purposes, the gain of the horn antenna without slots is also given (solid curve).

Due to symmetry, both configurations 1 and 2 give exactly the same patterns, which guarantee the radar radiation is not affected when switching the slots. The maximum gain is 15.93 dBi at $\theta = 90°$. As already discussed in Section 2, this is 1.3 dB less than for the horn antenna without any slot. Apart from this expected and controlled gain drop, the patterns are not disturbed compared to that of the reference antenna.

Figure 5 shows the gain patterns in xOy plane. In this case, the slots are responsible for an increase in side lobe level (in comparison to the horn without slots). Nevertheless, SLL remains lower than -18.66 dB, which is acceptable for many radar applications. Moreover, this SLL could easily be

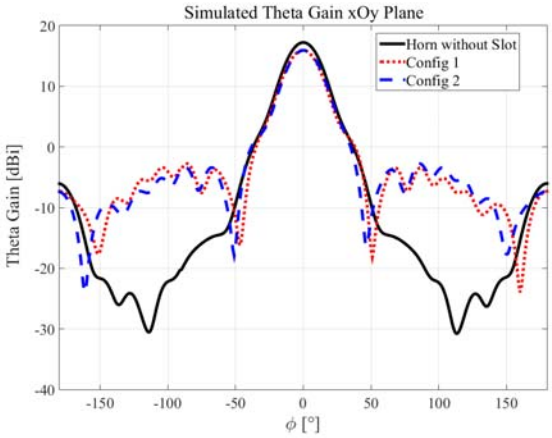

Figure 5. Comparison of simulated theta gains (radar function) in xOy plane at 5 GHz.

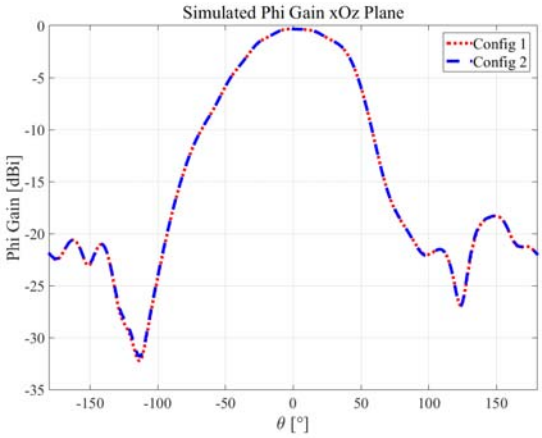

Figure 6. Comparison of simulated phi gains (communication function) in xOz plane at 5 GHz.

reduced further by using a smaller offset D (nonetheless at the expense of a lower power available for communication).

3.2. BPSK Communication at $\theta = 0°$

In this section, the performance of the communication antenna is analyzed. Fig. 6 presents the phi gain in xOz plane for configurations 1 and 2. This radiation, with orthogonal polarization and direction compared to that in the previous section, corresponds to the communication function.

As could be expected, the gain is identical for both configurations, and the maximum gain is reached at $\theta = 0°$. The quite low gain (-0.3 dBi) must not be misinterpreted. As the input power is supposed to be large (typically of many kW of peak power for an airborne radar, for example cf. [17]), the effective isotropic radiated power (EIRP) from the slot will be sufficient for communication purposes. In other words, the low value of the communication gain comes from the fact that the radiated power is normalized to the input power which is mostly devoted to the radar function. Moreover, the use of a non-directive radiating element such as a slot enables a large sectorial coverage on earth. In any case, the number of slots could be increased to improve the associated directivity. This could also be used to steer the beam if needed [18].

To go further, Fig. 7 superimposes the theta and phi gains in the xOz plane. It better highlights the achieved isolation between radar and communication functions. Two quantities can be defined to assess this isolation:

- The communication rejection corresponds to the rejection of phi polarization (due to communication function) in the radar direction ($\theta = 90°$, $\phi = 0°$).
- The radar rejection corresponds to the rejection of theta polarization (due to radar function) in the communication direction ($\theta = 0°$).

Note that the defined rejections correspond to cross-polar rejection (respectively in the communication and radar directions).

As can be observed, the radar rejection is 11 dB while the communication rejection is 37 dB. Table 1 summarizes the characteristics obtained for BPSK communication at $\theta = 0°$.

4. ANTENNA PROTOTYPE AND MEASUREMENT

4.1. Antenna Prototype

The prototype of the fabricated antenna is shown in Fig. 8. The antenna is made of AG3 with a thickness of 2 mm. A WR-187 waveguide ($47.55 \times 21.15\,\text{mm}^2$) operating from 3.95 to 5.85 GHz is used

Table 1. BPSK communication at 5 GHz and $\theta = 0°$ of direction of communication

Configurations	Phase (°)	Amplitude (dBi)
1	0	−0.3
2	180	−0.3

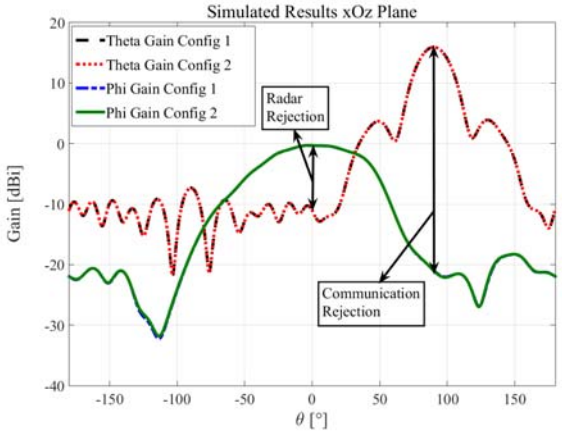

Figure 7. Simulated results of the multifunction antenna at 5 GHz in xOz plane.

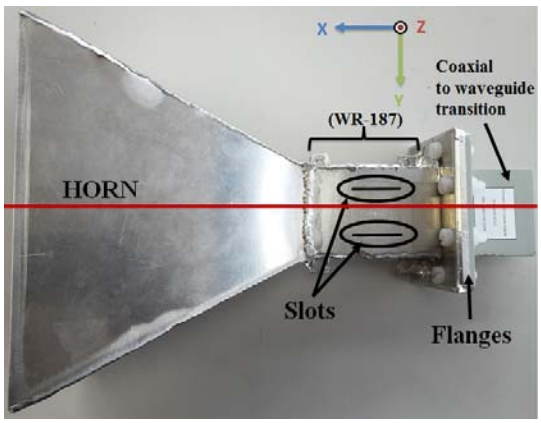

Figure 8. The multifunction antenna: prototype.

to feed the antenna system. The slot length was readjusted to be resonant at 5 GHz while taking into account the new thickness of the metal but also the flanges of the transition. An optimal radiation at 5 GHz is obtained for slot dimension $L = 29$ mm. In the next section, the simulations are redone considering the real thickness of the metallic walls and the new dimensions of the slots.

4.2. Measurement Results

Figure 9 shows the comparison of simulated and measured reflection coefficients of the two configurations. For each configuration, one of the slots was covered with copper tape. As can be seen, for all the studied configurations, the measured and simulated reflection coefficients are below

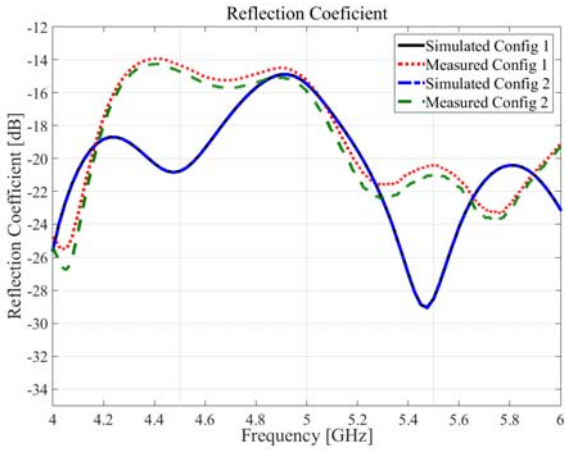

Figure 9. Comparison of simulated and measured reflection coefficients.

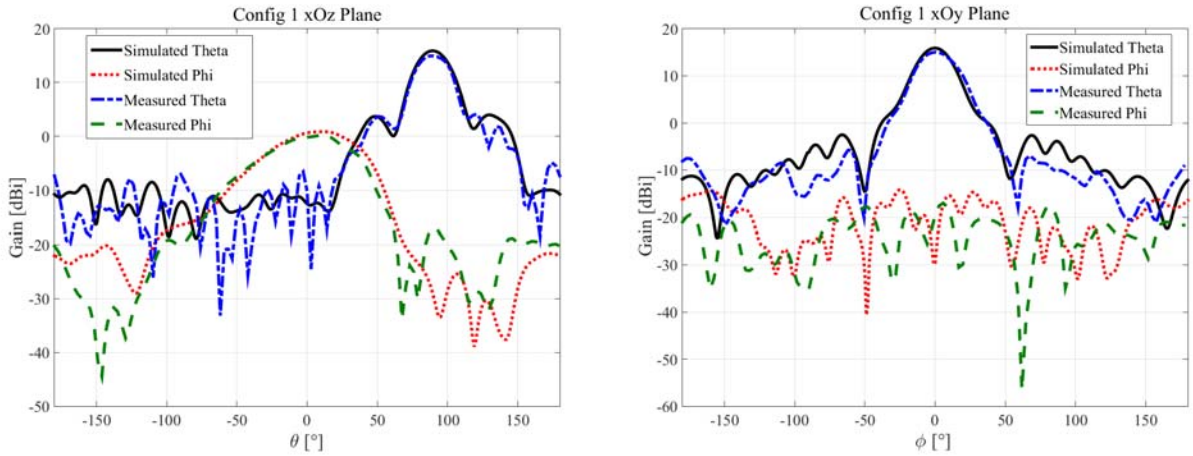

Figure 10. Comparison of configuration 1 simulated and measured gains at 5 GHz in xOz (a) and (b) xOy plane.

-14 dB from 4 to 6 GHz. The differences are due to the fabrication accuracy.

The simulated and measured gains at 5 GHz for configuration 1, in xOz and xOy planes, respectively, are plotted in Figs. 10(a) and (b). It can be observed that theta gains in simulation and measurement are in good agreement in the two planes. However, maximum theta gain is about 14.96 dBi for measurement and 15.9 dBi for simulation. This difference may be due to the measurement environment.

In xOz plane (Fig. 10(a)) simulated and measured phi gains present the same behavior for $\theta = [-50°, 50°]$ (corresponding to the phi gain main lobe). The radar rejection at $\theta = 0°$ (communication direction) is 9.5 dB for the measurement and 13 dB for the simulation. This degradation is the result of the appearance of oscillations in the side lobes region. Furthermore, at $\theta = 90°$ (radar direction), we notice an increase in the measured phi gain, but the communication rejection in this direction is 32 dB. The good isolation between radar and communication is confirmed by the low level of gain for polarization parallel along to the ϕ direction in xOy plane (Fig. 10(b)).

The measured gains in respectively xOz and xOy at 5 GHz of the two configurations are compared in Figs. 11(a) and (b). As expected, the main beam of the horn antenna used for radar function is

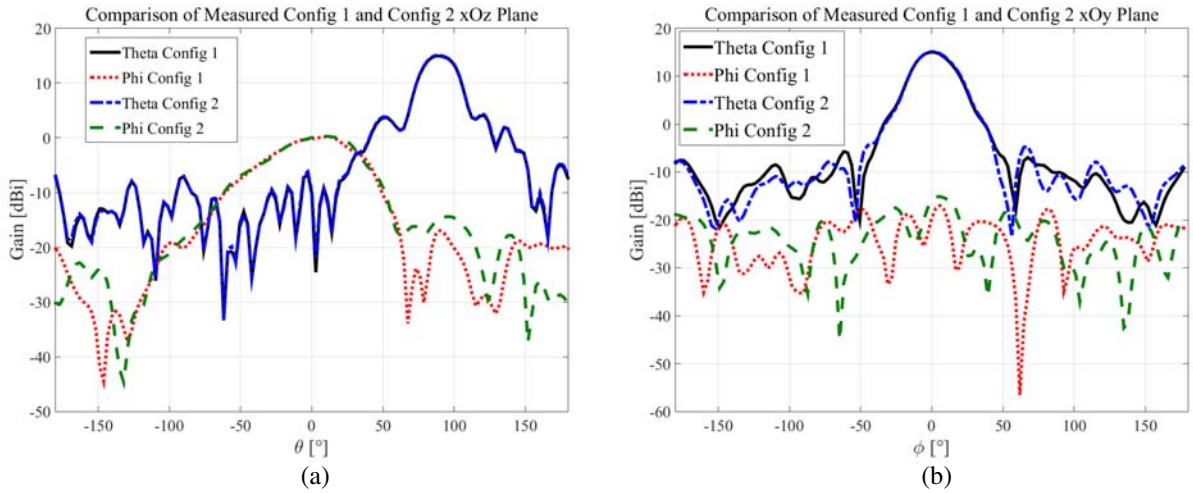

Figure 11. Comparison of configurations 1 and 2 of measured gains at 5 GHz in xOz (a) and (b) xOy plane.

identical for the two configurations in the two planes. This criterion is very important for the radar application since it guarantees that the radar function is not affected when switching for slot modulation. The slots radiations (phi gains) are also identical for the two configurations, in xOz plane (Fig. 11(a)) between $\theta = [-50°, 50°]$.

Figure 12 presents the measured phi gains at $\theta = 0°$ (corresponding to the communication direction) of the two configurations versus frequency. The -3 dB bandwidth of the communication function is 440 MHz, from 4.77 GHz to 5.21 GHz. In this frequency range, the difference between the phi gains is only 0.3 dB.

Figure 13 presents the measured theta gains at $\theta = 90°$, $\phi = 0°$ (corresponding to radar direction) of the two configurations versus frequency. As expected, the two configurations present the same behavior. At 5 GHz corresponding to the resonant frequency of the slot, the gain decreases due to the leakage in the slot for the communication function (see Section 2).

Figure 14 compares the measured radar rejections of the two configurations. At 5 GHz, it is 9.1 dB in the best case. However, when going away from the center frequency, the value decreases, reducing the operating bandwidth of the antenna system. This could be improved by using, for example, a

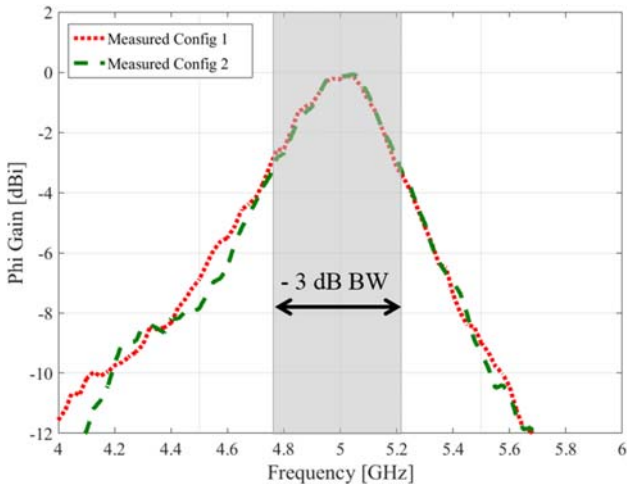

Figure 12. Measured phi gains (communication function) versus frequency ($\theta = 0°$, $\phi = 0°$).

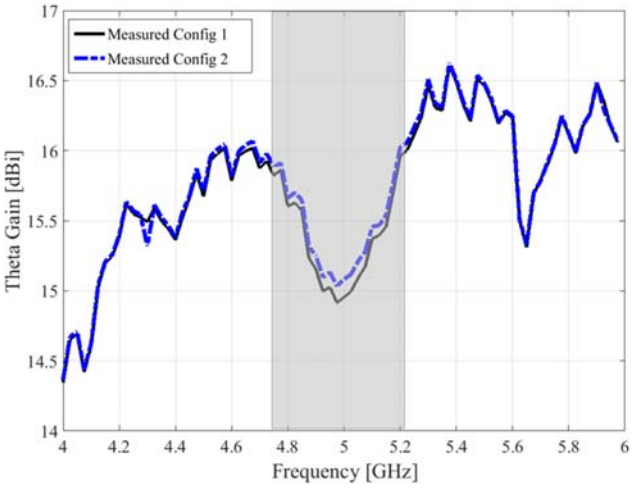

Figure 13. Measured theta gains (radar function) versus frequency ($\theta = 90°$, $\phi = 0°$).

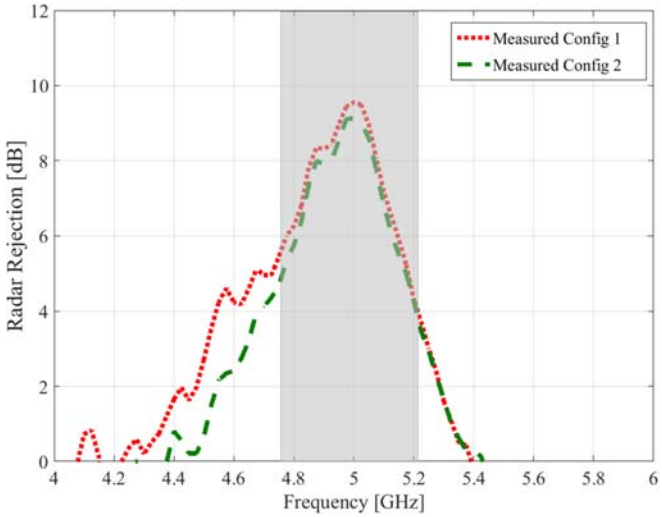

Figure 14. Measured radar rejection ($\theta = 0°$).

corrugated horn, which presents much lower side lobes than the standard horn.

Concerning the communication rejection ($\theta = 90°$, $\phi = 0°$), it is greater than 25 dB on the entire studied band, ensuring the isolation of radar and communication functions in this direction.

Table 2 summarizes the simulated and measurement results.

Table 2. Antenna results at 5 GHz

Designations	Simulated Results	Measured results
Horn gain	15.9 dBi	14.96 dBi
Radar Rejection	13 dB	9.1 dB
Communication Rejection	45 dB	32 dB

5. CONCLUSIONS

In this paper, a multifunction antenna providing a radar function and a communication function simultaneously through direct modulation has been proposed. A prototype has been built and measured. The system is composed of a horn antenna for radar purposes and a slotted waveguide for communication function. The system is designed so that the slots do not affect the operation of the main radar function. By using orthogonal polarizations and directions, the two functions operate simultaneously and do not interfere (at 5 GHz, the radar rejection is 9.1 dB in the communication direction and the communication rejection is larger than 25 dB in the radar direction). A direct BPSK modulation is achieved by switching between the two slots on the waveguide. The antenna system shows a good impedance matching (less than -14 dB) from 4 to 6 GHz for all the configurations, and the communication function -3 dB bandwidth is 440 MHz. Above all, the proposed antenna can be integrated with the existing radars using horns by replacing only the feeding waveguide.

REFERENCES

1. Renard, C. and M. Soiron, "Wideband multifunction airborne antennas," *2009 International Radar Conference "Surveillance for a Safer World" (RADAR 2009)*, 1–3, Bordeaux, France, Oct. 12–16, 2009.
2. Hou, Y., D. Su, W. Chen, and K. Ding, "Analysis and improvement the isolation between antennas on airborne platform with traveling wave antennas method," *Proc. IEEE Int. Symp. EMC Conference*, 1–4, Detroit, MI, USA, Aug. 18–22, 2008.
3. Hemmi, C., R. Thomas Dover, F. German, and A. Vespa, "Multifunction wide-band array design," *IEEE Trans. Antennas Propag.*, Vol. 47, 425–431, Mar. 1999.
4. Lemorton, J., C. Le Moine, C. Delhote, and F. Christophe, "Multifunction Antenna System Concepts: Opportunity for Ultra-wideband Radars?," *Non-standard Antennas*, Chap. 4, 93–100, J. Wiley and Sons, New Jersey, USA, 2011.
5. Quan, S. J., W. P. Qian, and J. H. Guo, "Radar-communication integration: An overview," *Proc. IEEE Int. Conf. Advanced Infocomm Technology (ICATT)*, 98–103, Fuzhou, China, Nov. 14–16, 2014.
6. Zhao, J., K. Huo, and X. Li, "A chaos-based phase-coded OFDM signal for joint radar-communication systems," *Proc. 12th ICSP*, 1997–2002, Hangzhou, China, Oct. 19–23, 2014.
7. Yue, Y. and J. Zhou, "A wideband dual-polarized antenna array for multifunction radar," *2016 IEEE 5th APCAP*, 393–394, Kaohsiung, Taiwan, Jul. 26–29, 2016.
8. Arismar Cerqueira, S. Jr., I. F. da Costa, S. Pinna, S. Melo, F. Laghezza, F. Scotti, P. Ghelfi, D. H. Spadoti, and A. Bogoni, "A novel dual-polarization and dual-band slotted waveguide antenna array for dual-use radars," *2016 10th EuCAP*, 1–4, Davos, Switzerland, Apr. 10–15, 2016.

9. Euzière, J., R. Guinvarc'h, R. Gillard, and B. Uguen, "Optimization of sparse time-modulated array by genetic algorithm for radar applications," *IEEE AWPL*, Vol. 13, 161–164, 2014.
10. Babakani, A., D. B. Rutledge, and A. Hajimiri, "Near-field direct antenna modulation," *IEEE Microwave Magazine*, 36–46, Feb. 2009.
11. Uhl, B., "Direct spatial antenna modulation for phased-array applications," *Proc. Int. Telemetering Conference*, Las Vegas, Nevada, USA, Oct. 2009.
12. Shanks, H. E. and R. W. Bickmore, "Four-dimensional electromagnetic radiators," *Canadian Journal of Physics*, Vol. 37, 263–275, 1959.
13. Ouedraogo, S., I. Hinostroza, R. Guinvarch, and R. Gillard, "Antenna system for simultaneous radar and communication applications," *2016 10th EuCAP*, 1–4, Davos, Switzerland, Apr. 10–15, 2016.
14. Ren, Y. J. and C.-P. Lai, "Wideband antennas for modern radar systems," *Radar Technology*, Chap. 17, InTech, 2010.
15. Kuriyama, A., H. Nagaishi, H. Kuroda, and K. Takano, "A high efficiency antenna with horn and lens for 77 GHz automotive long range radar," *2016 46th EuMC*, 1525–1528, London, England, Oct. 3–7, 2016.
16. FEKO v14, "Comprehensive computational electromagnetics (CEM) code," https://altairhyperworks.com/product/FEKO.
17. Conway, D., M. Fosberry, G. Brigham, E. Loew, and C. Liu, "On the development of a C-band active array frontend for an airborne polarimetric radar," *2013 IEEE Inter. Symp. on Phased Array Systems & Tech.*, 198–201, Waltham, MA, USA, Oct. 15–18, 2013.
18. Collin, R. E., "Aperture-type antenna," *Antennas and Radiowave Propagation*, Chap. 4, 265–273, McGraw-Hill, USA, 1985.
19. Kubo, H., M. Takamatsu, T. Yamamoto, and A. Sanada, "Waveguide-type discrete beam-scan antenna with switching diodes," *Proc. EuMC*, 1479–1482, Paris, France, Sept. 7–10, 2015.